MRS Advances © 2019 Materials Research Society
DOI: 10.1557/adv.2019.140

Effect of Ta addition on microstructure and mechanical properties of dual two-phase Ni_3Al-Ni_3V intermetallic alloy

Kazushige Ioroi, Yasuyuki Kaneno and Takayuki Takasugi

Department of Materials Science, Osaka Prefecture University, 1-1 Gakuen-cho, Naka-ku, Sakai, Osaka 599-8531, Japan

ABSTRACT

Mechanism for the hardening of two-phase Ni_3Al-Ni_3V intermetallic alloy to which 2 at.% Ta was added in different substitution manners for Ni, Al and V was presented, based on the microstructural observation, alloying behavior and lattice properties of the additive in the constituent phases. The hardening behavior was explained in terms of solid solution hardening in which the mixture rule in the volume fraction of the two constituent phases and the atomic size misfit evaluated from the changes of the lattice parameters were incorporated. Consequently, the hardening for the alloys in which the additives were substituted for Ni and V was attributed to solid solution hardening. On the other hand, the hardening for the alloy in which the additive was substituted for Al was attributed to the hardening due to microstructural refining in addition to the solid solution hardening.

INTRODUCTION

Following a unique microstructural feature of Ni base γ-γ ' type superalloys, so-called Ni base dual two-phase intermetallic alloys have been developed, based on the Ni_3Al ($L1_2$) and Ni_3V ($D0_{22}$) pseudo-binary alloy system shown in figure 1 [1,2]. At the hyper-eutectoid compositions, the microstructures at high temperatures are comprised of primary Ni_3Al phase (γ ') precipitated from Ni solid solution (γ) matrix. At low temperatures, the Ni solid solution existing in the channel region is transformed into a eutectoid microstructure consisting of the Ni_3Al and Ni_3V phases [3-5,6]. The microstructural stability is believed to be high at elevated temperatures because of crystallographically coherent microstructure between the two constituent phases, making the dual two-phase intermetallic alloys attractive as advanced high-temperature structural materials. In this study, tantalum (Ta) that stabilizes the two constituent phases [3] and is expected

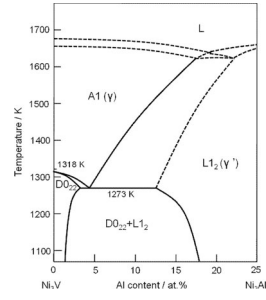

Figure 1. Phase diagram of the Ni_3V-Ni_3Al pseudo-binary alloy system constructed from our previous studies [1,2].

to behave as solid solution strengthener was added in different substitution manners for the constituent elements, Ni, Al and V of the dual two-phase intermetallic alloy. The atomic radius of Ta (0.147 nm) is larger than those of three constituent elements, Ni (0.125 nm), Al (0.143 nm) and V (0.137 nm) if defined by the Goldschmidt radius. First, microstructure, alloying (i.e. partition) behavior of Ta and lattice properties modified by Ta are investigated by a scanning electron microscope (SEM), an electron probe micro-analyser (EPMA) and X-ray diffraction (XRD). Next, hardness of the prepared alloys is measured at room temperature. Based on these experimental results, hardening behavior of the prepared alloys is discussed in terms of solid solution hardening and hardening due to microstructural refining.

EXPERIMENTAL PROCEDURES

A nominal composition expressed by 75Ni-10Al-15V (in at.%) was chosen as a base alloy. Ta at 2 at.% which is under the solubility limit was added to the base alloy, substituting each for Ni, Al and V. These alloys are referred to as 2Ta(*M*) alloy where the letter *M* between the parentheses indicates the constituent elements, Ni, Al or V substituted by Ta. Button ingots with 30 mm in diameter were prepared by arc melting in argon gas atmosphere using a non-consumable tungsten electrode on a copper hearth. They were solution-treated (homogenized) at 1553 K for 5 h in vacuum and then furnace-cooled at a rate of 10 K/min to room temperature.

Microstructural observation, elemental mapping and phase identification were performed with field emission (FE)-type SEM equipped with wave dispersive spectroscopy (WDS) and XRD. The XRD was performed using a Cu$K\alpha$ target. The XRD diffraction profiles for measuring accurate lattice parameters of the two constituent phases were drawn at a scanning speed of 0.1°/min. Since the observed reflection profiles were in many cases overlapped due to similar lattice parameters of the both constituent phases, accurate lattice parameters of the two constituent phases were determined, fitting the 220 reflection profile synthesized from the simulated 220_{Ni3Al}, 220_{Ni3V} and 204_{Ni3V} reflection profiles to the observed 220 reflection with a least discrepancy. The Vickers hardness test was performed in the conditions of a holding time of 10 s and a load of 1 kgf at room temperature. The hardness data of at least 10 points were averaged after excluding the largest and smallest values in each measurement.

RESULTS

Figure 2 shows the FESEM-secondary electron images (SEI) of the microstructures of the prepared alloys. The microstructure of the base alloy is composed of primary Ni_3Al precipitates and channel region. The precipitates tend to be aligned in direction normal to cube plane of the precipitates with somewhat cuboidal (square-like) morphology. On the other hand, the primary Ni_3Al precipitates in the 2Ta(Al) alloy were finer and more cuboidal than those of the base, 2Ta(Ni) and 2Ta(V) alloys. Also, the volume fraction of the primary Ni_3Al precipitates was the largest in the 2Ta(V) alloy, median in the 2Ta(Ni) alloy and the smallest in the 2Ta(Al) alloy (figure 3(a)). This rank appears to be reasonable, considering that the relative content of Al to V is increased in the 2Ta(V) alloy, unaffected in the 2Ta(Ni) alloy and reduced in the 2Ta(Al) alloy. The sizes of the primary Ni_3Al precipitates measured in volume (in m^3) are also plotted in figure 3(b). An interesting result is that the smallest size of the primary Ni_3Al precipitates was observed in the 2Ta(Al) alloy accompanied with a cuboidal morphology.

Regarding the partition behavior of Ta, the elemental distribution in the microstructure of the 2Ta(Ni) alloy is shown in figure 4. The Al-rich and V-rich region (corresponding to the channel region) are well separated for either alloy. It is evident that

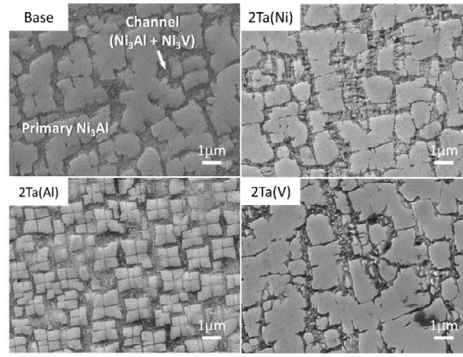

Figure 2. FESEM-secondary electron images (SEI) of the microstructures of the prepared alloys solution-treated at 1553 K for 5 h.

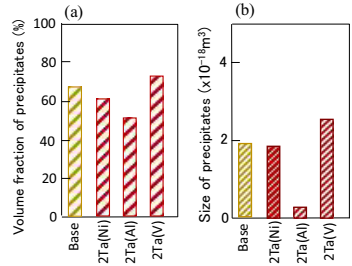

Figure 3. (a) Volume fraction, v_f and (b) size of the primary Ni_3Al precipitates in the microstructures of the alloys prepared in this study.

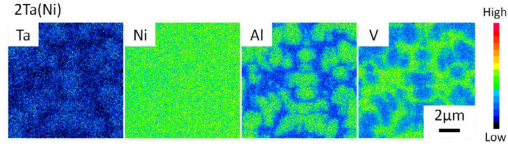

Figure 4. Elemental distribution in the microstructure of the 2Ta(Ni) alloy analyzed by FESEM-WDS.

Ta is enriched in the primary Ni_3Al precipitates. The partition coefficient $k_{Ta}^{L12/A1}$ of Ta was calculated to be 2.1, agreeing with the previous observation [1].

Determined lattice parameters (a, c') of the two constituent phases are plotted in figures 5 (a) and (b) where c' is a half of c. Those values are plotted on the horizontal axes scaled by Ta content dissolving in the two constituent phases. Also, the unit cell volume changes $|\Delta V|$ and $|\Delta V'|$ of the Ni_3Al and Ni_3V phases by the addition of 2 at.% Ta are plotted in figures 5 (c) and (d), calculating from figures 5 (a) and (b). It is found that the changes are larger in the substitution manner of Ta for Ni than for Al or V, irrespective of the constituent phase.

Figure 6 shows the Vickers hardness of the alloys prepared in this study. The hardness increase of the 2Ta(Al) alloy is larger in the substitution manner of Ta for Al than for Ni and V unlike the lattice expansion behavior.

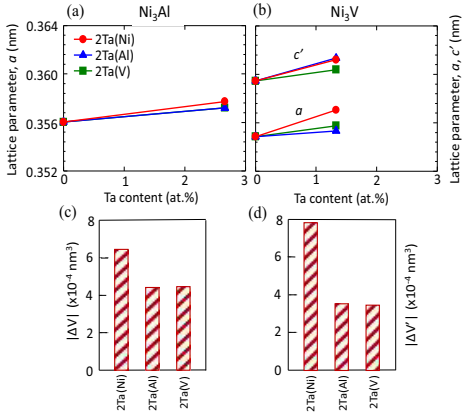

Figure 5. Changes of the (a,b) lattice parameters and (c,d) unit cell volumes in the (a,c) Ni_3Al and (b,d) Ni_3V phases for the alloys added with 2 at.% Ta.

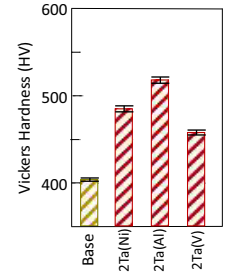

Figure 6. Vickers hardness of the prepared alloys solution-treated at 1553 K for 5 h.

DISCUSSION

The 2Ta(Al) alloy exhibited the microstructure with more cuboidal and finer Ni_3Al precipitates than the other alloys. Recent study on the γ-γ ' type superalloy showed that the morphology of the γ' precipitates became large and rounded when aging is performed at high temperatures after solid solution treatment and became fine and cuboidal when aging is performed at low temperatures [7]. The results were explained by energetic consideration: the morphology of the precipitates grown at high temperatures is governed by the 'surface energy' of the precipitate while those grown at low temperatures is governed by the 'elastic energy' involving the elastic strain energy due to the lattice mismatch between the precipitate and matrix and the elastic strain interaction energy between precipitates. The elastic energy is characterized by taking a negative minimum if the precipitates form cuboidal shape and are adjacent to each other along <100> direction [8,9]. It is widely recognized that the morphology of the individual precipitate is determined by minimizing the sum of the surface energy and elastic energy [10,11]. As a measure to predict which of the energy terms dominates in the present alloys, the solvus temperatures, T_s, at which the γ ' phase begins to precipitate during cooling after solid solution treatment were estimated from the phase diagrams of the Ni-Al-V ternary and Ni-Al-V-Ta quaternary alloys [1]. It was shown that the solvus temperature was lower for the 2Ta(Al) alloy than for the 2Ta(Ni) and 2Ta(V) alloys. Accordingly, it is suggested that the precipitation behavior in the 2Ta(Al) alloy is dominated by the elastic energy, resulting in fine and cuboidal precipitates aligned along <001> direction while that in the 2Ta(Ni) and 2Ta(V) alloys is dominated by the surface energy, resulting in large and rounded precipitates.

The lattice misfits between the Ni_3Al and Ni_3V phases were very small in either alloy, i.e., less than -0.25 % if defining the lattice misfit and -0.74 % if defining in the unit cell volume misfit. Thus, the crystal structures of the two constituent phases are quite coherent irrespective of the substitution manner of Ta.

The additional hardening from the base alloy by the Ta addition is attributed to the solid solution hardening due to Ta atoms dissolving in the two constituent phases and additionally to the hardening due to the microstructural refining. First, let us discuss the

former type of hardening. The solid solution hardening in binary alloys has been interpreted in terms of elastic interaction arising from atomic size and modulus misfits between solvent and solute atoms [12]. The flow stress increase in the concept of the elastic interaction is generally expressed in a form,

$$\Delta\tau = A\varepsilon^p C^q \tag{1}$$

Here A is constant, C is solute content. The term ε is the 'combined parameter' involving atomic size misfit defined by $(1/a)(\mathrm{d}a/\mathrm{d}C)$ and modulus misfit involving defined by $(1/G)(\mathrm{d}G/\mathrm{d}C)$ [12]. For the combined parameter, ε, the previous investigations [13,14,16] have shown that the atomic size misfit governs the solid solution hardening of Ni_3Al. Regarding the solid solution hardening of Ni_3V, no data for the parameters expressed in eq. (1) are unfortunately available up to date.

For the solid solution hardening ($\Delta\tau$) of the present two-phase alloys, the following assumption and approximation were taken: 1) similar solid solution hardening mechanism operates in the Ni_3Al and Ni_3V phases. 2) The mixture rule in the volume fractions, v_f and v_f', of the Ni_3Al and Ni_3V phases is incorporated. 3) For the combined parameter, ε, atomic size misfit parameters evaluated with $|(1/a_0)(\mathrm{d}a/\mathrm{d}C)|$ or $|(1/a_0^*)(\mathrm{d}a^*/\mathrm{d}C')|$ are assumed to dominate. Here, a_0 and a_0^* ($= \sqrt[3]{a \cdot a \cdot c'}$) are the lattice parameters of the Ni_3Al and Ni_3V phases in the base alloy, respectively. Here, C and C' are Ta contents dissolving in the Ni_3Al and Ni_3V phases, respectively, and 4) the parameter q is assigned to be 1, in accordance with the previously reported results for the Ni_3Al phase [13,14,15]. The constants, A involves Burgers vector and Poisson's ratio and have to be almost same in the both phases because same 1/2<110> type dislocations are activated in the both phases [16,17]. Therefore, the solid solution hardening (ΔHV) measured in hardness can be presented in an equation,

$$\Delta HV = K\left(\mu\left|\frac{1}{a_0}\frac{\mathrm{d}a}{\mathrm{d}C}\right|^p C v_f + \mu'\left|\frac{1}{a_0^*}\frac{\mathrm{d}a^*}{\mathrm{d}C'}\right|^p C' v_f'\right), \tag{2}$$

where the constant K involves the conversion factor from shear stress to Vickers hardness as well as Burgers vector and Poisson's ratio that were assumed to be identical in the both phases. In the calculation, the reported values, 77.0 GPa [18] and 97.3 GPa [19] were used for μ and μ', respectively. The values calculated from figures 5 (a) and (b) were used for the parameters, $|(1/a_0)(\mathrm{d}a/\mathrm{d}C)|$ and $|(1/a_0^*)(\mathrm{d}a^*/\mathrm{d}C')|$. The measured values were taken for the parameters, C and C' and the volume fractions, v_f and v_f'. The v_f is the volume fraction of the sum of the primary Ni_3Al phase and Ni_3Al phase present in the channel.

The solid solution hardening of the alloys was evaluated, plotting the hardness increment (from the base alloy), ΔHV, against the parameter calculated in eq. (2). The relation is shown in figure 7 in which p=1 was applied [20]. It is evident that ΔHV increases as the parameter in eq. (2) increases. The relation recognized by the 2Ta(Ni) and 2Ta(V) alloys was linear, passing through the origin in $\Delta HV-$ the parameter coordinate. On the other hand, the data point recognized by the 2Ta(Al) alloy was plotted in a higher ΔHV region, exceeding that recognized by the former alloys. This result means that the hardening responsible for the 2Ta(Ni) and 2Ta(V) alloys stems from the solid solution hardening while that responsible for the 2Ta(Al) alloy stems from the hardening due

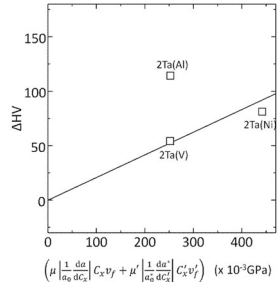

Figure 7. Relation between hardness increment, ΔHV and parameter calculated in eq. (2), after p=1.

to the microstructural refining in addition to the solid solution hardening.

CONCLUSIONS

The hardening behavior of the two-phase Ni_3Al-Ni_3V intermetallic alloy to which 2 at.% Ta was added in substitution manners for Ni, Al and V were studied by FESEM, EPMA, XRD and Vickers hardness. The following results were obtained from the present study.

(1) The alloy in which Ta was substituted for Al exhibited the microstructure with finer and more cuboidal Ni_3Al precipitates than the other alloys.
(2) The lattice expansion by the Ta addition was larger in the substitution manner for Ni than for Al or V in either constituent phase.
(3) The hardness increase by the Ta addition was larger in the substitution manner for Al than for Ni and V.
(4) The hardening of the 2Ta(Ni) and 2Ta(V) alloys was attributed to the solid solution hardening. The hardening for the 2Ta(Al) alloy was attributed to the hardening due to microstructural refining in addition to the solid solution hardening.

REFERENCES

[1] S. Kobayashi, K. Sato, E. Hayashi, T. Osaka, T.J. Konno, Y. Kaneno and T. Takasugi, Intermetallics **23**, 68 (2012).
[2] S. Semboshi, H. Tsuda, Y. Kanano, A. Iwase and T. Takasugi, Intermetallics **59**, 1 (2015).
[3] Y. Nunomura, Y. Kaneno, H. Tsuda and T. Takasugi, Acta Mater. **54**, 851 (2006).
[4] S. Shibuya, Y. Kaneno, M. Yoshida and T. Takasugi, Acta Mater. **54**, 861 (2006).
[5] S. Shibuya, Y. Kaneno, H. Tsuda and T. Takasugi, Intermetallics **15**, 338 (2007).
[6] T. Moronaga, Y. Kaneno, S. Semboshi and T. Takasugi, Phil. Mag. **95**, 3859 (2015).
[7] T. Takeshita, Y. Murata, N. Miura, Y. Kondo, Y. Tsukada and T. Koyama, J. Japan Inst. Met. Mater. **79**, 203 (2015).
[8] W.C. Johnson and J.K. Lee, Metall. Trans. A **10**, 1141 (1979).
[9] T. Miyazaki, H. Imamura, H. Mori and T. Kozakai, J. Mater. Sci. **16**, 1197 (1981).
[10] A. Kelly and R.B. Nicholson, Prog. Mater. Sci. **10**, 151 (1963).
[11] M. Doi, T. Miyazaki and T. Wakatsuki, Mater. Sci. Eng. **67**, 247 (1984).
[12] L.A. Gypen and A. Deruyttere, J. Mater. Sci. **12**, 1028 (1977).
[13] R.W. Guard and J.H. Westbrook, Trans. Met. Soc. AIME **215**, 807 (1959).
[14] R.D. Rawlings and A.E. Staton-Bevan, J. Mate. Sci. **10**, 505 (1975).
[15] Y. Mishima, S. Ochiai, N. Hamao, M. Yodogawa and T. Suzuki, Trans JIM **27**, 648 (1986).
[16] T. Moronaga, Y. Kaneno, H. Tsuda and T. Takasugi, Mater. Sci. Forum **706-709**, 1077-1082 (2012).
[17] K. Hagihara, M, Mori, T. Kishimoto and Y. Umakoshi, Mater. Sci. Forum **638-642**, 1318-1323 (2010).
[18] H. Yasuda, T. Takasugi and M. Koiwa, Acta Metall. Mater. **40**, 381 (1992).
[19] Y. Zhao, L. Qi, Y. Jin, K. Wang, J. Tian and P. Han, J. Alloys Compounds **647**, 1104 (2015).
[20] F.R.N. Nabarro, Phil. Mag. **35**, 613 (1977).